Article published online: 2023-08-11

Correction of Angular Limb Deformities in Two Dogs Using a Conformation-Based Surgical Approach and Planning Software

Tyler J. Wyatt[1] Albert C. Lynch[2]

[1] Cornell University College of Veterinary Medicine, Ithaca, New York, United States
[2] Albert Charles Lynch Surgery LLC, Philadelphia, Pennsylvania, United States

Address for correspondence Albert C. Lynch, BVM&S, DACVS, Albert Charles Lynch Surgery LLC, Philadelphia, PA 19350, United States (e-mail: albert.c.lynch@gmail.com).

VCOT Open 2023;6:e84–e92.

Abstract

The aim of this study is to describe a novel conformation-based approach to surgical planning and execution, as well as novel orthopaedic planning and rehearsal software. This report presents two cases of angular limb deformity correction, utilizing a novel conformation-based technique. A combination of computed tomography and radiographs was used to characterize the deformities for each case. Case 1 presented with a biapical deformity of the left antebrachium. Case 2 presented with deformities affecting the left femur and tibia. Rendering of a three-dimensional (3D) bone model, surgical planning, and production of multistep surgical jigs were executed using a traditional mesh-modeling workflow for case 1, whereas case 2 utilized the described novel software. No intraoperative complications were encountered while using the surgical kits. The multistep surgical jigs facilitated major procedural steps with precision, including application of definitive fixation. The novel software reduced the surgical planning time and the operator's requirement for 3D modeling skill. All osteotomies were stabilized in compression with acceptable alignment and good patient outcomes. This novel conformation-based approach and planning software, developed by the corresponding author, may provide an alternative method of correcting canine angular limb deformities. Further research on this technique and software is indicated before commercial availability.

Keywords
- conformation based
- patient specific
- three-dimensional printing
- angular limb deformity
- planning software

Introduction

Computer modeling and three-dimensional (3D) printing in orthopaedics continues to evolve. Traditional uses include preoperative planning, surgical education, and procedure rehearsal.[1–3] Development of intraoperative patient-specific guides (PSG) and surgical equipment has been reported.[3–12] Advantages of PSG include improved surgical precision, reduced intraoperative decision-making, and reduced intraoperative radiation.[7–14]

Correction of angular limb deformities (ALD) is a common application of this technology. Current techniques require the operator to manually derive and handle data related to the bone's conformation, creating potential sources of geometric inaccuracy. First, the operator must characterize the bone's alignment through acquisition of objective measurements from diagnostic imaging. Then, the operator must replicate these measurements, as well as the bone's three orthogonal planes and joint planes, in the 3D mesh file that results from rendering of the computed tomography (CT)

received
January 30, 2023
accepted after revision
May 24, 2023

DOI https://doi.org/10.1055/s-0043-1771233.
ISSN 2625-2325.

Georg Thieme Verlag KG, Rüdigerstraße 14, 70469 Stuttgart, Germany

data. Error can also exist as the operator attempts to elucidate the true plane and magnitude of the deformity and generate a surgical guide within the mesh file. A mathematically derived bone template capable of generating a functional 3D rendering, based on the bone's objective conformational parameters, as well as automatically produce a surgical guide of interest, may minimize the possible sources of error.

Patient-specific guides, as produced via the conventional workflow, use unique, typically juxta-articular, bony topographic landmarks to ensure appropriate spatial orientation. The surgical approach associated with exposure of these landmarks may negatively impact blood supply, implant positioning, and bone healing, and be a source of postoperative morbidity. Development of a workflow that generates guides that are not specific to the bone's surface topography may mitigate these adverse effects, as well as expand their spatial and functional versatility.

Computed tomography is a prerequisite for generation of PSG and equipment. The degree to which PSG conforms to a patient's topographic anatomy is impacted by CT slice thickness[15] and the use of smoothing algorithms. These drawbacks are in addition to time, radiation exposure, and cost implications associated with CT. A technique that does not require advanced multiplanar imaging in the development of surgical equipment may be beneficial.

Here, we describe a novel, conformation-based surgical planning (CBSP) approach and modeling software that aims to address these aforementioned limitations.

Materials and Methods

Medical and surgical planning records (January 2019–August 2022) of dogs undergoing ALD correction were reviewed. Cases eligible for inclusion were dogs that presented for a lameness or mechanical dysfunction secondary to an ALD and underwent correction using a novel CBSP approach. Of the cases that met the inclusion criteria, the two cases presented in this report were selected to juxtapose traditional mesh modeling and the developed software. Case 1 demonstrates the approach using traditional mesh modeling (stl file). Case 2 demonstrates the capability of the developed software to semiautomate the process using computer-aided design (CAD) modeling (SLDPRT file). All procedures were planned and performed by the corresponding author.

To characterize the deformity and define the bone alignment parameters, a combination of preoperative CT (Aquilion 64 slice, 1.0-mm slice thickness, Toshiba, Tokyo, Japan) and orthogonal radiographs were utilized. Bone conformation was described using objective alignment parameters including joint orientation angles, bone length, bone width at various locations, and center of rotation of angulation (CORA; ►**Figs. 1A and 2A**). Torsion and joint rotation were assessed using established techniques with CT,[16,17] if available, or via goniometry if radiographs were used alone. Case 2 had an incomplete CT scan of the affected femur, without ability to repeat the imaging study; therefore, the magnitude of femoral neck anteversion, and torsion, had to be estimated.

A 3D rendering of the affected bone was then generated, with the operator-measured alignment parameters visibly imposed on it. The rendering was generated as a mesh file (stl) from the available CT scan for case 1, with the objective parameters being manually reproduced by the operator. For case 2, to generate a true-CAD-based bone model template (SLDPRT file) for the software developed by the corresponding author (viewed in SolidWorks, Dassault Systems), a skeleton framework is created that consists of orthogonal sketch planes, joint planes, deformation planes, and anatomical or mechanical axes. The solid body surfaces are then created as the spatial dimensions are detailed. Skeleton and surface sketches are mathematically linked, with established orthopaedic trigonometric functions controlling their interactive user functions. These skeleton and surface components are alterable via a data sheet, enabling the templates to reflect different breeds and species, as well as introduce or correct deformations for a given template. The bone template mathematic functions can automatically calculate and display the true plane and magnitude of the deformity, based on the objective parameters disclosed by the operator. The bone template is also capable of being placed in an assembly (SLDASM file), with template osteotomies, guides, and jig components selected by the operator, to create a multistep surgical jig as a semiautomated process.

After the conformational parameters have been imposed on the 3D rendering, the virtual osteotomies are planned and multistep jigs modeled using the CBSP technique (►**Figs. 3** and **4**).

The patients were premedicated with dexmedetomidine (3 µg/kg IV) + hydromorphone (0.1 mg/kg IV), induced with propofol (4 mg/kg IV to effect), and maintained with isoflurane. Intraoperative complications as it relates to the surgical technique were categorized into complications with assembly of the printed components or postoperative radiographs revealing osteotomies that are not well apposed, as this would indicate a discrepancy between the planned and performed procedure. Objective outcomes were evaluated postoperatively, while subjective patient outcomes were evaluated at 6 months postsurgery.

Case 1 (►**Figs. 1** and **3**): A 1-year old, 20-kg, male neutered mixed chondrodystrophic dog presented with a biapical deformity and negative ("short ulna") radioulnar incongruity affecting the left antebrachium and associated moderate weight bearing lameness. Preoperative CT was performed followed by 3D rendering (stl file) using imaging software (Horos; Nimble Co LLC, Annapolis, Maryland, United States). Postprocessing of the mesh file was then performed (MeshMixer; Autodesk, San Francisco, California, United States) so that the virtual 3D model could be imported into mesh modeling software (►**Fig. 1B**; TinkerCad; Autodesk). Orthogonal planes, joint axes, joint planes, and conformationally objective parameters were manually replicated for the mesh model using multiplanar reformation (MPR) and radiographs as reference. The true plane and magnitude of the deformity was derived and additionally imposed on

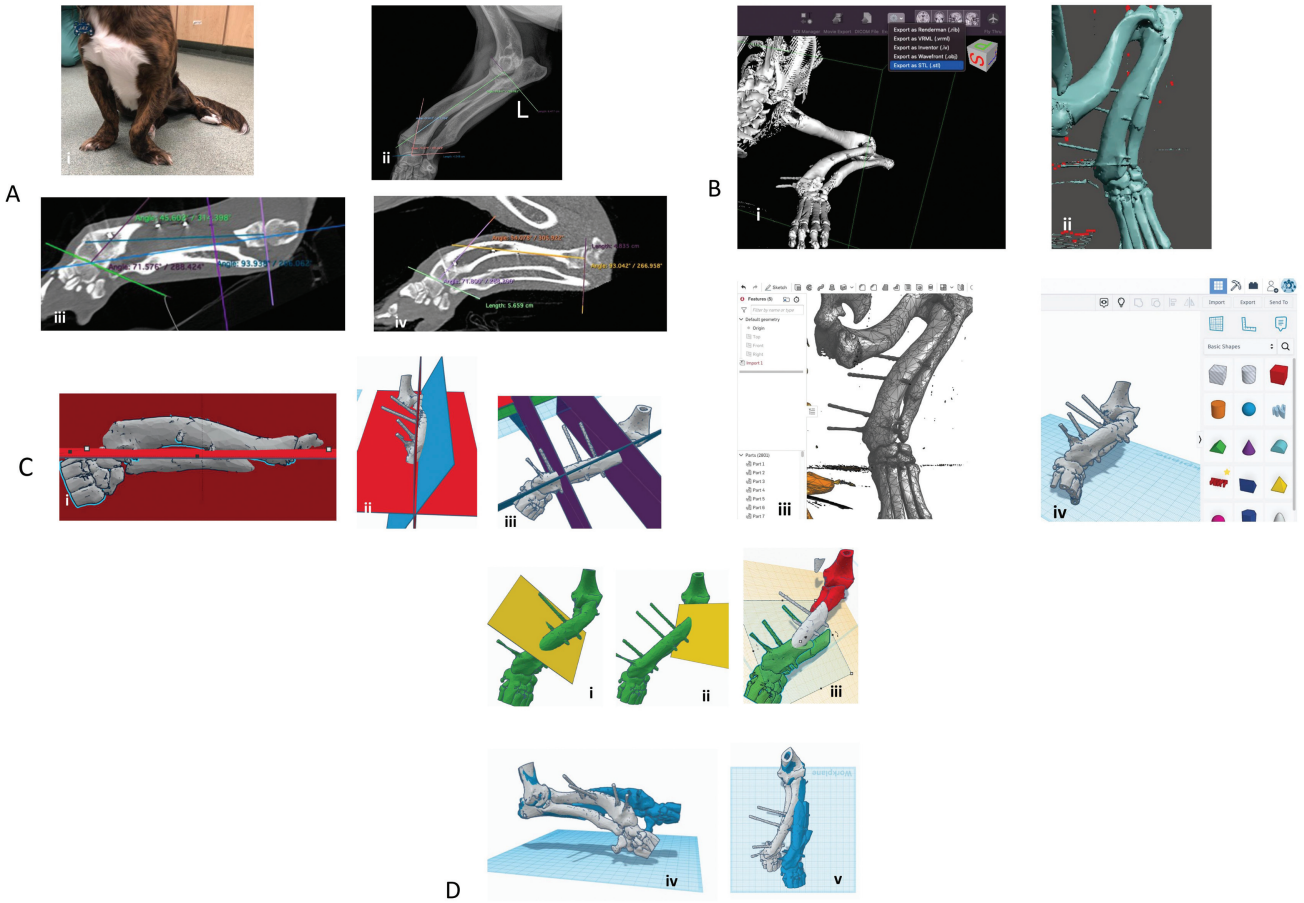

Fig. 1 *Case 1*. Steps required to obtain three-dimensional (3D) rendering of a bone and perform virtual osteotomies using traditional mesh modeling. Note: Two K-wire marker pin sets may be observed protruding from bone (**B**–**D**). (**A**) Image acquisition. The patient presents with deformity (i). Conformation-specific parameters are defined, which can be achieved using radiographs (ii) and/or computed tomography (CT) imaging (iii and iv). Multiplanar reformation (MPR) images (iii and iv) give the user true orthogonal perspective; however, there may be differences in the parameters measured even between two adjacent "slices." The magnitude of deformity in image (iii) compared with (iv) is 10 degrees. This can leave the user searching for the MPR views that best "match" conformation-specific parameters obtained via radiography (ii), which would be (iii) in this example. (**B**) 3D rendering and image post-processing. The medical data viewing software used can generate and export a 3D mesh file render of the CT data (i). This file is then segmented and analyzed within software capable of these postprocessing steps (ii). Once processed, the mesh file can be imported into computer modeling software (iii, iv). True computer-aided design (CAD) software (iii; Onshape, Boston, Massachusetts, United States) is heavily based on model-based definition (MBD), wherein the model itself contains sufficient data constraints and functions to fully define said model. Because true CAD parametric and MBD modeling is not possible in such CAD software, the mesh file is imported into mesh modeling software (ii, iv) for interaction. The software selected (iv) for modeling the surgical components has smaller file sizes and faster computer rendering times. (**C**) Replicating and imposing the conformationally specific parameters on the mesh file. Orthogonal, thin surfaces are made within the mesh modeling software and manually positioned (i) such that they replicate the sagittal and frontal planes observed within the MPR images (**Fig. 1Aiii**). The joint orientation planes have been removed for visualization purposes, but the *red planes* in (i) and (ii) represent sagittal and frontal planes. Trigonometric oblique planar analysis is used to determine the true plane, the *blue plane* in (ii) and (iii), and magnitude of deformity. Centers of rotation of angulation (CORA) location(s) are manually imposed, based on those objective conformationally specific parameters elucidated via the initial diagnostic imaging. At the location of those imposed CORA, the transverse bisecting line (TBL) may be defined perpendicular to the true plane. TBLs are seen as the *purple planes* in (iii). (**D**) Selecting and virtually rehearsing the proposed osteotomies. Bi-oblique sliding osteotomies were chosen; therefore, the plane of the osteotomy, seen as *yellow planes* in (i) and (ii) are deviated from the TBL. The mesh model is cut along the osteotomy planes, resulting in three independent sections that are translated into the desired state of alignment (iii). Start and end alignment may be seen in (iv) and (v) as *gray* and *blue mesh models*, respectively.

the mesh model and bi-oblique sliding osteotomies were planned virtually.[18]

All steps of the CBSP procedure and modeling were performed manually, with case 1 utilizing traditional mesh modeling. Alterations to the surgical 3D printed components required manual update of the entire model. To assist in the accuracy of the modeling process, two 0.045-in K-wire sets were placed during the preoperative CT in a location representing two pin sets. The third pin set was planned virtually and surgically placed in the mediolateral plane of the proximal radius, without fiducials, using the other pin sets to attach a pin set guide. All 3D printed equipment was printed using nylon filament (CR10s pro; Creality, Shenzhen, China) and steam sterilized.

A standard craniolateral approach to the left radius was made. The fiducial K-wires were overdrilled with a cannulated drill bit and the two associated pin sets inserted with affiliated handles. These two pin sets and handles were

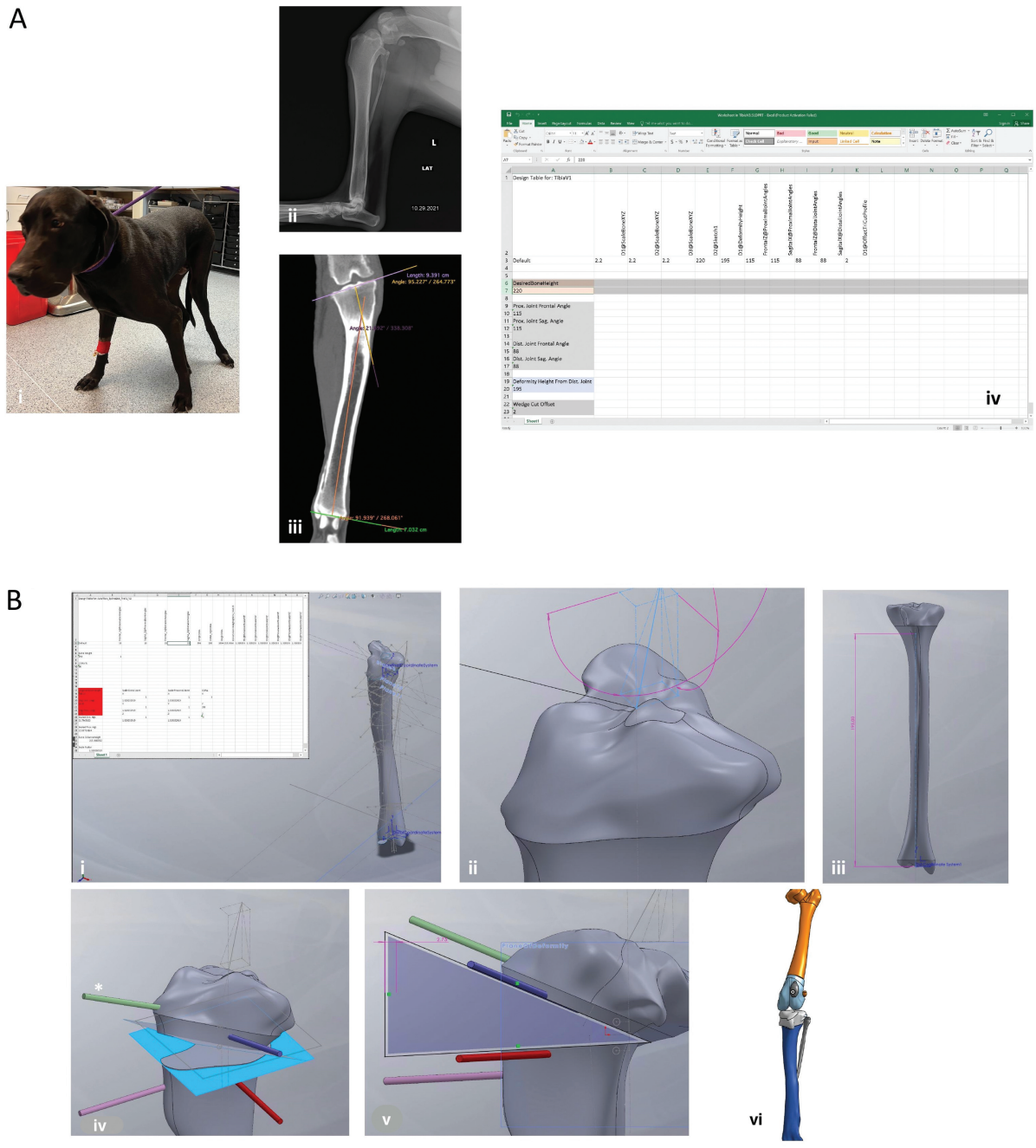

Fig. 2 *Case 2*. Steps required to obtain a three-dimensional (3D) rendering of a bone and perform virtual osteotomies with realignment using the developed software. Descriptive reference to the tibia exhibited to highlight software functionality. Note that computer-aided design (CAD) "pins" (*) seen in (**B**) are placed automatically by the software and are available for subsequent modeling (see ►**Fig. 4**). (**A**) Acquisition and disclosure of conformation parameters. The patient presents with deformity (i). Initial efforts are to define the conformationally specific parameters using planar radiographs (ii) ± computed tomography (CT) imaging (iii). These conformationally specific parameters are inserted into excel design table (iv), thereby fully constraining the associated CAD file. This CAD file is in model-based definition (MBD) template of a normal tibia, based on cited normal parameters in the literature, and the only constraints missing from the equation are fulfilled upon the user defining the previously described conformationally specific parameters. (**B**) Automated CAD rendering. The CAD template bone exists as mathematically defined planes and sketches (i) and (ii), such that once the conformational parameters are entered within the excel design table, a de novo 3D rendering of a dimensionally equivalent normal bone is produced (i). This rendering does not utilize any shape modeling, point distribution or registration techniques, and it is fully defined and constrained. As such, the user can simply enter the level of the deformity into the excel design table to define the planned level of the osteotomy (iii). Once the conformational parameters specific to the magnitude of deformity observed in each of the orthogonal planes are inserted within the design table, the CAD file automatically generates a de novo 3D rendering of the deformed bone with the true plane and magnitude of the deformity revealed (iv) and (v). Virtual rehearsal and alterations to the CAD file are rapid and robust (vi), without risk of human error aside from the parameters detailed within the design table.

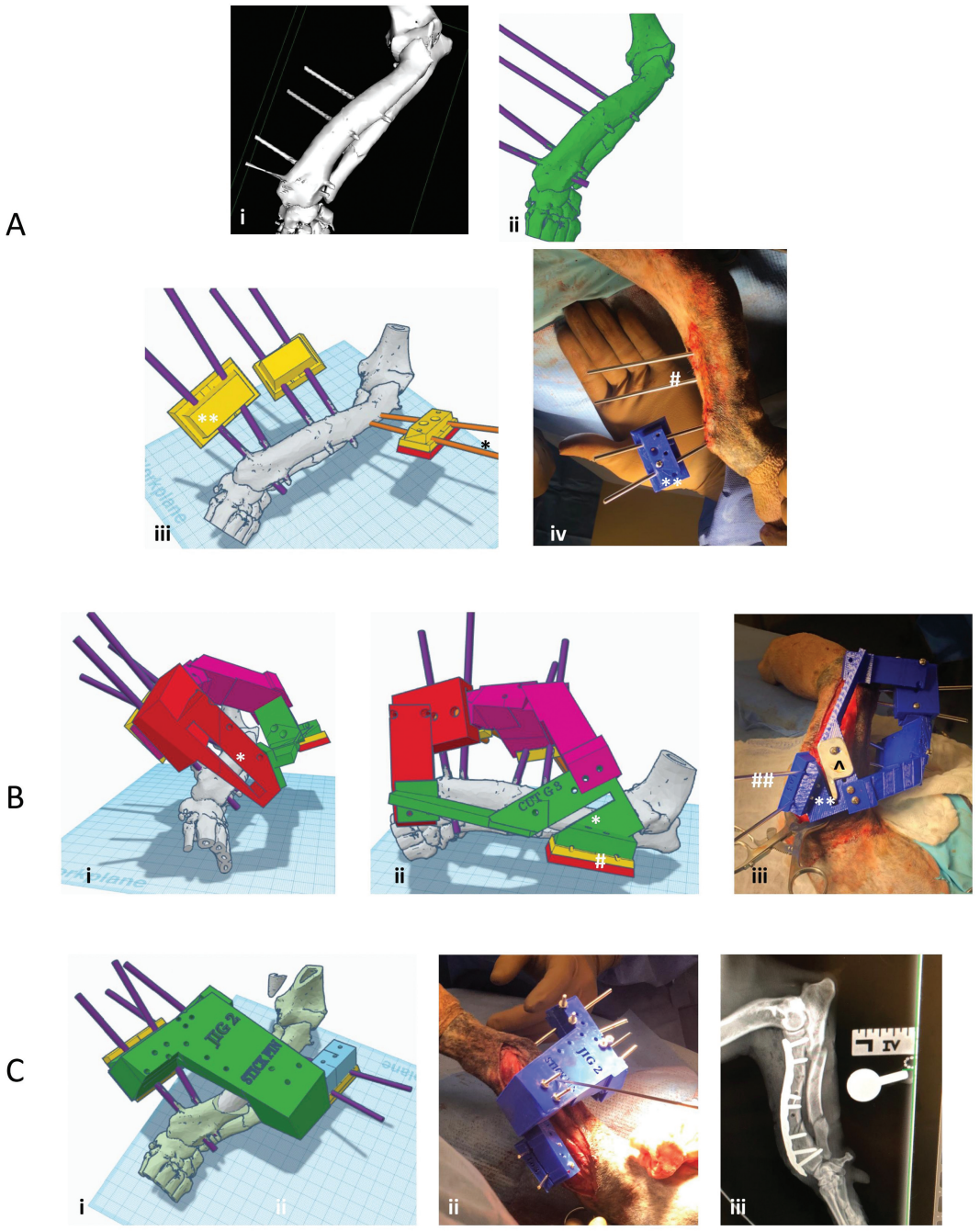

Fig. 3 *Case 1*. Steps required to model and utilize the surgical components using traditional mesh modeling. (**A**) Pin set placement. For each bone segment to be isolated, a pin set was virtually implanted. The K-wires initially used for reference registration (i) are manually replicated and replaced with mesh model Steinmann pins (ii). A pin set handle is modeled with a stand-off distance from the bone surface (iii), which may be achieved via nonparallel pin sets, mechanical stops on the pins, or a physical spacer. Pin set handles have a unique shape that allows them to attach, detach, and reattach various jigs and guides. Each handle guides a pin set in a locally arbitrary orientation related to the engaged bone segment, but globally specific orientation, as it relates to the deformed bone. As such, pin sets must be placed simultaneously so that the global relationship to one another, and their engaged bone segments, is specific to the deformity. The virtual pins match the size of the pin (#) that will be used at surgery (iv) to attach to the pin set handle (**). A third pin set was required in this case that had no reference K-wire pin set present and was therefore modeled virtually (*) for future insertion via the initial pin placement jig (see series B). (**B**) Pin placement jig and cutting guides. A rigid pin placement jig securing all three pin handles, and corresponding pin sets, was modeled (i and ii) and used in surgery (iii). The jig ensures maintenance of global relationship if all associated pin sets engage bone bicortically. The pin set distal to the osteotomy is positioned relative to the proximal pin set with a spatial relationship that mimics the deformity. The location where the third pin set was modeled (#) and successfully placed at surgery (##). The pin placement jig also had two cutting guides modeled (*) that were enclosed on at least three sides and can be seen at surgery (**). The metal shield (^) can be seen secured to the cutting guide to avoid any fragments from the 3D components from forming. Cutting guides are modeled to attach to either a pin set handle or a jig. (**C**) Final alignment jig and implant guide. After virtual osteotomies have been performed and bone segments realigned, a repositioning jig was modeled that attaches to each pin set handle. This jig translates each bone segment via their corresponding pin set into final alignment and also has jig plate positioning and drill guides to facilitate placement of precontoured implants for definitive fixation. The final alignment jig can be seen modeled (i) and in surgery (ii). Postoperative lateral radiograph shows final alignment (iii).

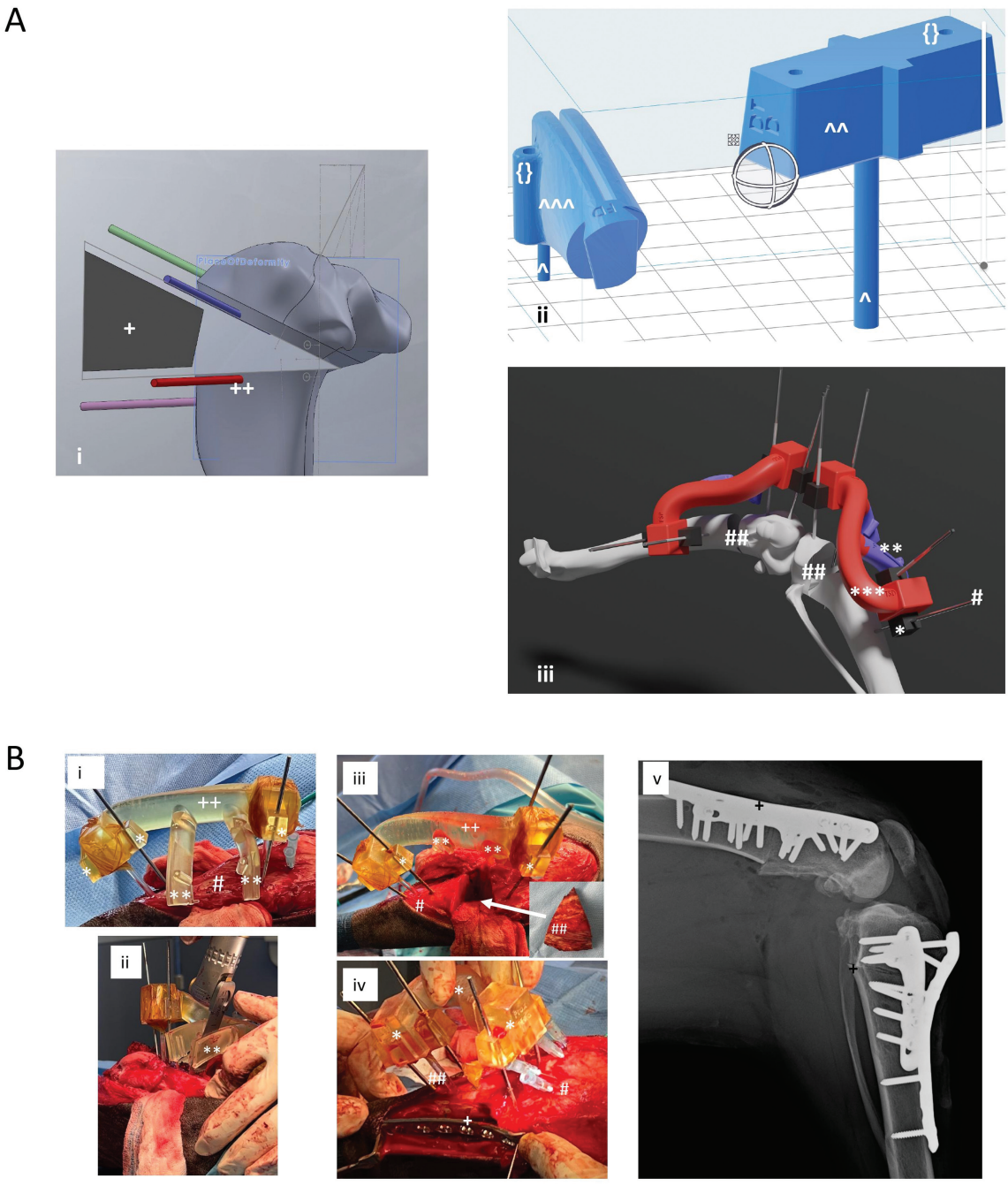

Fig. 4 *Case 2*. Steps required to model and utilize the surgical components using the developed software. (**A**) Pin placement jig and cutting guides (no fiducial marker used). (i) The true magnitude of the deformity is propagated in the true plane of the deformity to automatically generate a basic osteotomy (+). Locoregional pin placement is automatically offered (++). Both the pins placed and the complexity of the cutting guide may be altered by the operator depending on needs and preference. (ii) A cutting guide (^^^) and the pin handle (^^) that it is modeled to attach to are seen with their stand-off guides (^) to ensure precision spatial relation to the bone surfaces, and subsequent pin set insertion. In this image, the cutting guide is enclosed on three sides, and a pin guide ({}) is seen. Both components have drafted dovetail slots, affording modular mating capability. Labels help ensure proper modular mating and orientation. (iii) The entire component assembly is seen for the pin placement jig. Pin handles (*), cutting guides (**), pin placement jig (***), and pins (#). Planned closing wedge ostectomy sites (##) of the femur and tibia. The pin placement jig is modeled to attach to each pin handle, the first of which ensures maintenance of global relationship if all associated pin sets engage bone bicortically. The pin set distal to the osteotomy is positioned relative to the proximal pin set with a spatial relationship that mimics the deformity. (**B**) Components used at surgery and postoperative lateral radiograph. (i) Patient bone (#), pin placement jig (++), pin handles (*), and cutting guides (**). (ii) Use of cutting guide (**) at surgery. (iii) Patient bone (#), pins and pin handle (*), site of detached cutting guides (**), and excised bone section (##). (iv) Patient bone (#) and final alignment jig (*) translating bone to desired end position. Internal fixation implant (+). Stand-off guide (##). (v) Lateral radiograph of patient tibia and femur showing desired alignment and osteotomy apposition along with internal fixation devices. After osteotomies have been performed and bone segments realigned, the final alignment jig translates each bone segment via their corresponding pin set into final alignment. Placement of precontoured implants for definitive fixation is facilitated by incorporation of jig plate positioning and drill guides.

attached to the pin placement jig, which guided the third pin set in the mediolateral plane of the proximal radius, as well as the bi-oblique sliding osteotomies that were planned at each CORA. Once the two osteotomies were complete, the pin placement jig was removed so that the alignment jig could be attached to the three pin set handles, thereby translating each of the three bone segments into their planned alignment state. This alignment jig also guided the placement of definitive internal fixation.

Case 2 (►**Figs. 2** and **4**): A 3-year-old, 45-kg, female spayed Great Dane presented with bilateral deformities affecting the femurs and tibiae, with concurrent grade 4 lateral patellar luxation and associated moderate weight bearing lameness. Surgical correction of the left femur and tibia was elected, as it was the clinically more affected side. Preoperative CT was performed on the tibia, but a complete study of the femur was not available. Orthogonal radiographs and the available MPR views of the left tibia and femur were used to obtain available conformational parameters. These parameters were then detailed to the developed software, which then updates the conformation of the 3D rendered bone template to reflect those parameters. Among these disclosed parameters included the level and measured magnitude of deformity, the operator's preferred osteotomy technique, and pin set positions. This enabled the software to automatically reveal the true plane and magnitude of the deformity, as well as produced the surgical jigs as a semiautomated process. The orthogonal planes, joint axes, joint planes, conformational parameters, CORA, and selected osteotomies were automatically executed through the encoded mathematical algorithm. All steps of the CBSP procedure and modeling were completed as an automated function. It was elected to simultaneously level the tibial plateau, given concern for cranial cruciate ligament disease. The operator may give feedback to the program to modify the pin set positions, shape of the construct, or any other aspect in a parametric manner that automatically updates every aspect of the modeled construct. All 3D printed equipment was printed using surgical guide resin (Form 3B; Formlabs) and steam sterilized.

A standard medial approach to the proximal tibia was made, followed by a medial arthrotomy. The tibial triangulating pin placement jig was placed using the incorporated pin set stand-off posts to maintain appropriate spatial orientation of the apparatus. The closing wedge osteotomy guides were attached to execute the ostectomy. The triangulating pin placement jig was removed, and the realignment jig attached, thus realigning the tibial bone segments to their planned alignment orientation and to guide definitive fixation. This process was repeated for the femoral triangulating jig, closing wedge ostectomy, realignment, and placement of definitive fixation, from a medial approach. The left femur and tibia each had closing wedge osteotomies performed at the level of their CORA. A recession trochleoplasty was performed.

Results

The CBSP process took approximately 20 hours for case 1 and approximately 1 hour for case 2. For both cases, there were not any intraoperative complications, all components of the multistep surgical jigs were successfully employed, and surgical time was approximately 3 hours.

Case 1 underwent postoperative physiotherapy for 3 months after surgery and reported an excellent long-term subjective outcome by the owner. Case 2 did not pursue postoperative physiotherapy and reported a good long-term subjective outcome by the owner.

All available postoperative alignment parameters were within 3 degrees of the planned outcome (►**Table 1**).

Table 1 Preoperative, virtually planned, and postoperative alignment parameters for cases 1 and 2

Case no.	Preoperative	Planned virtually	Postoperative
1	aMPRA 52° aLDRA 47° aCdPRA 90° aCdDRA 68° Procurvatum 42° Torsion 33°	aMPRA 61° aLDRA 75° aCdPRA 98° aCdDRA 77° Procurvatum 30° Torsion 16°	aMPRA 62° aLDRA 73° aCdPRA 98° aCdDRA 73° Procurvatum 32° Torsion[a]
2	FNA[a] mLPFA 90°[b] mLDFA 70°[b] mMPTA 118° mMDTA 101° TPA 23° mCrDTA 82° Tibia torsion 0°	FNA[a] mLPFA 95° mLDFA 95° mMPTA 95° mMDTA 95° TPA 5° mCrDTA 82° Tibia torsion 0°	FNA[a] mLPFA 93° mLDFA 97° mMPTA 98° mMDTA 98° TPA 4° mCrDTA 82° Tibia torsion 0°

Abbreviations: aCdDRA, anatomical caudal distal radial angle; aCdPRA, anatomical caudal proximal radial angle; aLDRA, anatomical lateral distal radial angle; aMPRA, anatomical medial proximal radial angle; FNA, femoral neck anteversion; mCrDTA, mechanical cranial distal tibial angle; mLPFA, mechanical lateral proximal femoral angle; mLDFA, mechanical lateral distal femoral angle; mMPTA, mechanical medial proximal tibial angle; mMDTA, mechanical medial distal tibial angle; TPA, tibial plateau angle.

[a]Insufficient imaging data to report.

[b]Estimated due to incomplete imaging data.

Discussion

Here, we present a novel CBSP technique and software for correcting two cases of canine ALD. This CBSP technique is centered on defining the aberrant spatial relationships among the main segments of a deformed bone. Rather than depending on anatomical landmarks for spatial calibration of the 3D bone rendering during the computer modeling process, this CBSP technique employs principles of triangulation, enabling the surgeon to produce multistep surgical jigs that facilitate numerous aspects of the ALD corrective surgery. Therefore, the CBSP technique may prove to be a versatile technique, with a wide patient population, to complement the current PSG technique.

The novel orthopaedic planning and rehearsal software used in case 2 demonstrates that a conformationally precise 3D rendering of a long bone may be produced without CT and has the potential to reduce error associated with the human operator during the computer modeling process. Additionally, the software *dramatically reduces the CBSP process*, obviates the barrier of the operator needing to know mesh or CAD modeling, and facilitates generation of surgical kits that can semiautomate the corrective surgery. While further studies are needed for validation, this technique may provide advantages that could advance the field of surgical 3D printing and modeling.

To perform the CBSP technique, the alignment and conformation parameters of a presenting limb must be objectively described by the operator, allowing for spatial calibration within the selected mesh or CAD modeling software. These parameters may be obtained via orthogonal radiographs, CT imaging, mesh model analysis, or any other means the operator prefers. For case 1, those parameters were manually replicated within the mesh model (►**Fig. 1**). Case 2 used the developed software, enabling the user to access a mathematically derived template bone that is fully constrained upon input of those conformational parameters, producing a 3D rendering (►**Fig. 2**). These parameters, which could be obtained via radiographs alone, are therefore all that is needed to generate a 3D rendering and surgical aid components when utilizing the developed software. Further studies are underway to demonstrate the accuracy of these renderings when compared with 2D and 3D outcome measures.

With a representative 3D model of the deformity generated, corrective osteotomies can be planned by locating and defining any CORA. In case 1, CT digital imaging and communications in medicine (DICOM) and MPR measurements were converted to the CORA location on the mesh file. Planes created in this file can then be used to direct the location of osteotomy (►**Fig. 1B–D**). This process was time intensive due to the manual calculation and replication of each step. In case 2, CAD automates the process as the surgeon operator provides the orthogonally measured magnitude of deformity and level of CORA, and the true plane of deformity and its magnitude are calculated. Osteotomies can then be planned with minimal user involvement, potentially reducing human error risk during the planning process.

Once corrective osteotomies are planned, modeling of complete surgical kits can reduce error risk associated with translating rehearsal surgery outcomes to the patient. In case 1, this process was time intensive, taking multiple days, as the operator had to manually manipulate spatial relationships among modeled components (►**Fig. 3**). In case 2, modeling took less than 1 hour, as the component library within the CAD assembly scaled upon user input and was positioned based on pin set locations (►**Fig. 4**). Because the CAD template is controlled by established trigonometric constraints for long bone deformities, this occurs automatically as the surgeon inputs the level of the CORA, magnitude of deformity observed, and measured torsional deformity, making any alterations rapid and free of operator error risk. Further studies are indicated to evaluate its efficacy with surgeons with varying experience levels.

Ensuring that pin sets placed in the bone match, the exact spatial relationship and insertion plane as what was virtually planned is critical to modeling complete surgical kits. In case 1, K-wires inserted prior to CT served as fiducial markers for the first pin sets to be placed. Additional pin sets can then be planned virtually and placed at surgery (►**Fig. 3B**). This evolved into all pin sets being planned virtually and placed at surgery, as in case 2. This is accomplished using a triangulating starting jig containing pin sets with spacers that offset the kit from the bone to ensure appropriate spatial orientation of the apparatus, minimize surgical footprint, and preserve blood supply (►**Fig. 4**). Additional anesthetic episodes and morbidity associated with fiducial K-wires are avoided.

Surgical kits are modeled to the needs of the deformity, and may include triangulating jigs, osteotomy guides, alignment jigs, drill guides, pin guides, and plate insertion guides that allow every step after pin insertion to be a semiautomated process. *This allows major steps of the surgery to be virtually planned, modeled, and printed*. Once fabricated, the tactile feedback provided by proper fit of mated components ensures that the bone beneath the skin is in the desired position when the appropriate guide is used. Because there is minimal tolerance for printed components to mate unless pin sets and engaged bone segments are in appropriate spatial configuration, the surgeon is afforded stepwise feedback once the pin set placement jig is placed appropriately. In both cases, surgical kits were constructed at surgery without complication, postoperative osteotomies were well apposed, and implants positioned appropriately (►**Figs. 2B** and **4B**). Uncomplicated surgical kit use, along with postoperative alignment parameters closely reflecting planned alignment parameters, demonstrates that the patient surgeries mimicked their virtual rehearsals. Further studies evaluating the accuracy and precision of both the CBSP technique and planning software are indicated.

In addition to advantages afforded by PSG, there are complementary advantages that a CBSP approach may offer. These include an *expanded patient population* and case application, *possibility of* less invasive approaches, and development of complete surgical multistep jigs that facilitate precise and repeatable outcomes. Further, the described

software has the potential to reduce the existing 3D modeling skill requirement, significantly expedite the planning process, reduce the requirement for preoperative CT, and minimize error risk associated with the human operator. Limitations associated with the CBSP technique, and planning software, include the need for further evaluation of objective outcome parameters and development of templates for various breeds with different predicted conformations. Such research is indicated before commercial availability. Despite these limitations, as well as those additional limitations discussed throughout the Discussion section, continued use and development of the presented technology may yield a practical, dependable, and versatile method of correcting limb deformities.

Disclosure

The developed software is a proprietary and patented software under the corresponding author.

Funding

None.

Conflict of Interest

None declared.

References

1 Rengier F, Mehndiratta A, von Tengg-Kobligk H, et al. 3D printing based on imaging data: review of medical applications. Int J CARS 2010;5(04):335–341
2 Harrysson OLA, Cormier DR, Marcellin Little DJ, Jajal K. Rapid prototyping for treatment of canine limb deformities. Rapid Prototyping J 2003;9(01):37–42
3 Giannatsis J, Dedoussis V. Additive fabrication technologies applied to medicine and health care: a review. Int J Adv Manuf Technol 2007;40(1–2):116–127
4 Hoang D, Perrault D, Stevanovic M, Ghiassi A. Surgical applications of three-dimensional printing: a review of the current literature & how to get started. Ann Transl Med 2016;4(23):456
5 Hamilton-Bennett SE, Oxley B, Behr S. Accuracy of a patient-specific 3D printed drill guide for placement of cervical transpedicular screws. Vet Surg 2018;47(02):236–242
6 Phan K, Sgro A, Maharaj MM, D'Urso P, Mobbs RJ. Application of a 3D custom printed patient specific spinal implant for C1/2 arthrodesis. J Spine Surg 2016;2(04):314–318
7 Oxley B. A 3-dimensional-printed patient-specific guide system for minimally invasive plate osteosynthesis of a comminuted mid-diaphyseal humeral fracture in a cat. Vet Surg 2018;47(03):445–453
8 Worth AJ, Crosse KR, Kersley A. Computer-assisted surgery using 3d printed saw guides for acute correction of antebrachial angular limb deformities in dogs. Vet Comp Orthop Traumatol 2019;32(03):241–249
9 Oxley B. Bilateral shoulder arthrodesis in a Pekinese using three-dimensional printed patient-specific osteotomy and reduction guides. Vet Comp Orthop Traumatol 2017;30(03):230–236
10 Hall EL, Baines S, Bilmont A, Oxley B. Accuracy of patient-specific three-dimensional-printed osteotomy and reduction guides for distal femoral osteotomy in dogs with medial patella luxation. Vet Surg 2019;48(04):584–591
11 Easter TG, Bilmont A, Pink J, Oxley B. Accuracy of three-dimensional printed patient-specific drill guides for treatment of canine humeral intracondylar fissure. Vet Surg 2020;49(02):363–372
12 Kim J, Song J, Kim SY, Kang BJ. Single oblique osteotomy for correction of congenital radial head luxation with concurrent complex angular limb deformity in a dog: a case report. J Vet Sci 2020;21(04):e62
13 Crosse KR, Worth AJ. Computer-assisted surgical correction of an antebrachial deformity in a dog. Vet Comp Orthop Traumatol 2010;23(05):354–361
14 Altwal J, Wilson CH, Griffon DJ. Applications of 3-dimensional printing in small-animal surgery: A review of current practices. Vet Surg 2022;51(01):34–51
15 Webster CE, Marcellin-Little DJ, Koballa EM, Stallrich JW, Harrysson OLA. Evaluation of the geometric accuracy of computed tomography and microcomputed tomography of the articular surface of the distal portion of the radius of cats. Am J Vet Res 2019;80(10):976–984
16 Kroner K, Cooley K, Hoey S, Hetzel SJ, Bleedorn JA. Assessment of radial torsion using computed tomography in dogs with and without antebrachial limb deformity. Vet Surg 2017;46(01):24–31
17 Aper R, Kowaleski MP, Apelt D, Drost WT, Dyce J. Computed tomographic determination of tibial torsion in the dog. Vet Radiol Ultrasound 2005;46(03):187–191
18 Youngman J, Raptis D, Al-Dadah K, Monsell F. An accurate method of determining a single-plane osteotomy to correct a combined rotational and angular deformity. Strateg Trauma Limb Reconstr 2015;10(01):35–39

